Molecular Therapy
Oncolytics
Original Article

A Novel Aurora Kinase Inhibitor Attenuates Leukemic Cell Proliferation Induced by Mesenchymal Stem Cells

Jun-Dan Wang,[1,6,7] Wei Zhang,[2,7] Jing-Wen Zhang,[1] Ling Zhang,[1] Le-Xun Wang,[1] Hong-Sheng Zhou,[5] Liang Long,[4] Gui Lu,[4] Quentin Liu,[1,3] and Zi-Jie Long[1]

[1]Department of Hematology, The Third Affiliated Hospital, Sun Yat-sen University; Institute of Hematology, Sun Yat-sen University, Guangzhou 510630, China; [2]Department of Clinical Immunology, The Third Affiliated Hospital, Sun Yat-sen University, Guangzhou 510630, China; [3]Sun Yat-sen University Cancer Center; State Key Laboratory of Oncology in South China, Guangzhou 510060, China; [4]Institute of Medicinal Chemistry, School of Pharmaceutical Sciences, Sun Yat-sen University, Guangzhou 510006, China; [5]Department of Hematology, Nanfang Hospital, Southern Medical University, Guangzhou 510510, China; [6]Department of Hematology, Guangdong Provincial People's Hospital, Guangdong Academy of Medical Sciences; School of Medicine, South China University of Technology, Guangzhou 510080, China

Acute myeloid leukemia (AML) mesenchymal stem cells (MSCs) play an essential role in protecting leukemic cells from chemotherapeutic agents through activating a wide range of adhesion molecules and cytokines. Thus, more attention should be paid to attenuate the protection of leukemic cells by MSCs. By examining the gene expression files of MSCs from healthy donors and AML patients through high-throughput microarrays, we found that interleukin (IL)-6 was an important cytokine secreted by AML MSCs to protect leukemic cells, contributing to disease progression. Strikingly, Aurora A (AURKA) was activated by IL-6, offering a new target to interfere with leukemia. Importantly, a novel AURKA inhibitor, PW21, showed excellent AURKA kinase inhibitory activities and attenuated the interaction of leukemic cells and the microenvironment. PW21 inhibited MSC-induced cell proliferation, colony formation, and migration, and it induced cell apoptosis. Mechanically, PW21 could inhibit IL-6 secreted by MSCs. Moreover, we found that PW21 displayed a strong anti-leukemia effect on non-obese diabetic (NOD)-severe combined immunodeficiency (SCID) and murine MLL-AF9 leukemic models. PW21 significantly prolonged the survival of leukemic mice and eliminated the leukemic progenitor cells. AURKA inhibitor PW21 could provide a new approach for treatment of leukemia through blocking the protection by the leukemic microenvironment in clinical application.

INTRODUCTION

The acute myeloid leukemia (AML) bone marrow (BM) microenvironment is an important part of disease progression and pathophysiology, among which, mesenchymal stem cells (MSCs) play an essential role in the activation of alternative survival signaling pathways, protecting leukemic cells from chemotherapeutic agents. Much of the interaction between leukemic cells and MSCs occurs through a wide range of adhesion molecules on leukemic cells and their corresponding ligands secreted by the MSCs.[1,2] Aurora A (AURKA) was abnormally expressed in malignancies, including solid tumors and leukemia.[3] Our study showed that expression of AURKA was markedly elevated in BM mononuclear cells (BMMCs) obtained from a significant portion of AML patients.[4] Importantly, previous reports have shown a distinctive gene-expression profile of MSCs of AML patients compared with MSCs of healthy donors, and they revealed that proteoglycans and adhesion molecules, metabolic pathways, endocytosis pathways, cytokine-cytokine receptor interactions, and chemokine signaling were deregulated in AML BM-MSCs.[5] AURKA mRNA was expressed at significantly higher levels in MSCs from myelodysplastic syndrome (MDS) patients when compared with hematopoietic cells and healthy donors. The presence of chromosomal abnormalities (mainly aneuploidy) in hematopoietic cells/MSCs was also associated with higher levels of AURKA.[6,7]

Small-molecule kinase inhibitors of AURKA have attracted a great interest, such as MLN8054, MLN8237, and ENMD-2076, which are being investigated in clinical trials.[8] MLN8237 is a second-generation compound and the first that was bioavailable orally, which was evaluated against multiple myeloma (MM), chronic myeloid leukemia (CML) expressing nonmutated and mutated forms of BCR-ABL, peripheral T cell lymphomas (PTCLs), and other solid tumors.[9–11] A

Received 17 March 2020; accepted 27 July 2020;
https://doi.org/10.1016/j.omto.2020.08.001.

[7]These authors contributed equally to this work.

Correspondence: Zi-Jie Long, Department of Hematology, The Third Affiliated Hospital, Sun Yat-sen University; Institute of Hematology, Sun Yat-sen University, Guangzhou 510630, China.
E-mail: longzij@mail.sysu.edu.cn
Correspondence: Quentin Liu, Department of Hematology, The Third Affiliated Hospital, Sun Yat-sen University; Institute of Hematology, Sun Yat-sen University, Guangzhou 510630, China.
E-mail: liuq9@mail.sysu.edu.cn
Correspondence: Gui Lu, Institute of Medicinal Chemistry, School of Pharmaceutical Sciences, Sun Yat-sen University, Guangzhou 510006, China.
E-mail: lugui@mail.sysu.edu.cn

phase II study of MLN8237 in AML and MDS revealed that MLN8237 induced leukemic cell senescence.[12] MLN8237 has been in phase III clinical trials and tested in patients with relapsed or refractory PTCLs (ClinicalTrials.gov: NCT01482962). We previously showed that our new designed AURKA inhibitor, AKI603, could inhibit leukemia cell proliferation and colony formation both *in vitro* and *in vivo*,[13,14] suggesting the potential application of targeting AURKA in hematologic malignancies.

While the effects of the microenvironment on AML have been extensively investigated, little attention has been paid to the effects of targeted inhibitors, especially AURKA inhibitors, on the AML microenvironment. In this study, we investigated the signaling pathways of MSCs in the AML microenvironment and found that a novel AURKA inhibitor, PW21, could significantly inhibit MSC-induced cell proliferation and colony formation, suggesting its new application in AML microenvironment intervention.

RESULTS

Gene Expression Patterns of MSCs Are Explored between Healthy Donors and AML Patients

To address possible signaling in the interaction between the stromal microenvironment and leukemic cells, we first examined the gene expression patterns from three healthy donors (hBM-MSCs) and four AML patients (AML-MSCs, Table S2). hBM-MSCs and AML-MSCs were isolated, purified, and characterized for mesenchymal markers, including CD90 and CD105 expression (Figure 1A). A differentially expressed gene was defined as a gene whose absolute $\log_2$fold change (FC) of the differential expression is greater than or equal to 1 and the p value is less than 0.05. According to this standard, the volcano map of significantly different expression of mRNAs is shown in Figure S1A. We found that 552 mRNAs were upregulated while 390 mRNAs were downregulated in AML-MSCs compared with hBM-MSCs. To test whether the identified molecules are biologically meaningful, Gene Ontology (GO) and the Kyoto Encyclopedia of Genes and Genomes (KEGG) were used for function enrichment analysis. GO used three aspects to describe gene set functions, including biological process (BP), molecular function (MF), and cellular component (CC). Modules in regulation of actin cytoskeleton organization showed upregulated by BP-GO, while the nucleotide-binding oligomerization domain (NOD)-like receptor and nuclear factor κB (NF-κB) signaling pathways were increased by KEGG among the significantly upregulated mRNAs (Figures 1B and 1C; Figure S1B). As shown in the heatmap in Figure 1D, genes that mediated cell adhesion, such as ICAM1, and molecules activated in NF-κB signaling pathways, such as interleukin (IL)-1β, KLF5, TRAF5, and TLR4, were found to be elevated in the AML-MSCs. Western blot further confirmed that NF-κB/p65 and ICAM1 expression were increased in AML-MSCs compared with hBM-MSCs as expected (Figure 1E). Notably, gene set enrichment analysis (GSEA) found that AML-MSCs showed a significant enrichment of genes that are related to the cellular response to interferon (IFN)-γ, cell-matrix adhesion, and IL-6 production, whereas cell cycle checkpoint, collagen metabolic process, and hematopoietic stem cell differentiation signaling were downregulated (Figure 1F). Furthermore, we showed that RELA (NF-κB) displayed significant Pearson's correlation with IL-6 (Figure 1G). Our data suggested that NF-κB and IL-6 signaling might play an important role in the AML microenvironment protecting leukemic cells from chemotherapeutic agents.

AML-MSCs Promote Proliferation and Colony Formation of Leukemic Cells

In order to investigate how the stromal microenvironment supported the survival of leukemic cells, cells were cultured with conditioned medium (CM) from AML-MSCs and hBM-MSCs for 48 h and subjected to cell counting. The result showed that AML-MSC CM induced cell proliferation significantly compared with hBM-MSC CM both in NB4 and HL-60 cells (Figure 2A). A colony-forming unit (CFU) assay also revealed that AML-MSC CM clearly increased the number and the diameter of colonies (Figures 2B and 2C). A cell adhesion assay was performed by co-culture of MSCs with leukemic cells. The hBM-MSC co-cultured leukemic cells exhibited less adhesion to MSCs than did AML-MSC co-cultured leukemic cells (Figure 2D). Then, we examined the long-term effect of CM on cell survival capacity. To this end, the two cell types were subjected to AML-MSC CM or hBM-MSC CM for 6 days, and a Sytox Green stain assay was used to detect cell death. We found that after co-culture, AML-MSC CM protected cells from death but not hBM-MSC CM (Figure 2E). Moreover, gene expression patterns in AML-MSC or hBM-MSC co-cultured leukemic cells were further determined. Surprisingly, GO analysis showed that downregulated genes were enriched in positive regulation of cytokine production and regulation of inflammatory response-related pathways in AML-MSC CM co-cultured leukemic cells (Figure 2F). Thus, we examined the expression of ICAM1, IL-6, and IL-1β in MSC CM co-cultured leukemic cells by real-time PCR. The results showed that ICAM1, IL-6, and IL-1β were all decreased in the AML-MSC CM group (Figure 2G). Next, AML-MSC CM or hBM-MSC CM co-cultured leukemic cells were injected to the nude mice and the result showed that both tumor weight and volume were increased in the AML-MSC CM co-cultured leukemic cell group (Figures 2H and 2I). All of the above results suggested that MSCs offered a stromal microenvironment to support the survival of leukemic cells.

Inhibition of AURKA by PW21 Overcomes MSC-Induced Malignancy

IL-6 activation stimulated NF-κB expression, contributing to cancer development,[15] and we previously reported that AURKA regulated the NF-κB signaling pathway to promote cancer cell survival.[16] We next investigated whether IL-6 secreted by MSCs was the mediator for leukemic cell survival. Of note, IL-6 induced AURKA kinase activation (Figure 3A) and induced cell proliferation and migration in both NB4 and HL-60 cells (Figures 3B and 3C). In another independent work, we have designed and synthesized a novel AURKA inhibitor PW21 with a quinazoline skeleton (chemical structure shown in Figures S2A and S2B), which showed excellent AURKA kinase inhibitory activity, with the 50% inhibitory concentration (IC_{50}) value of 6.0 nM, while the inhibitory activity to Aurora B (AURKB) is

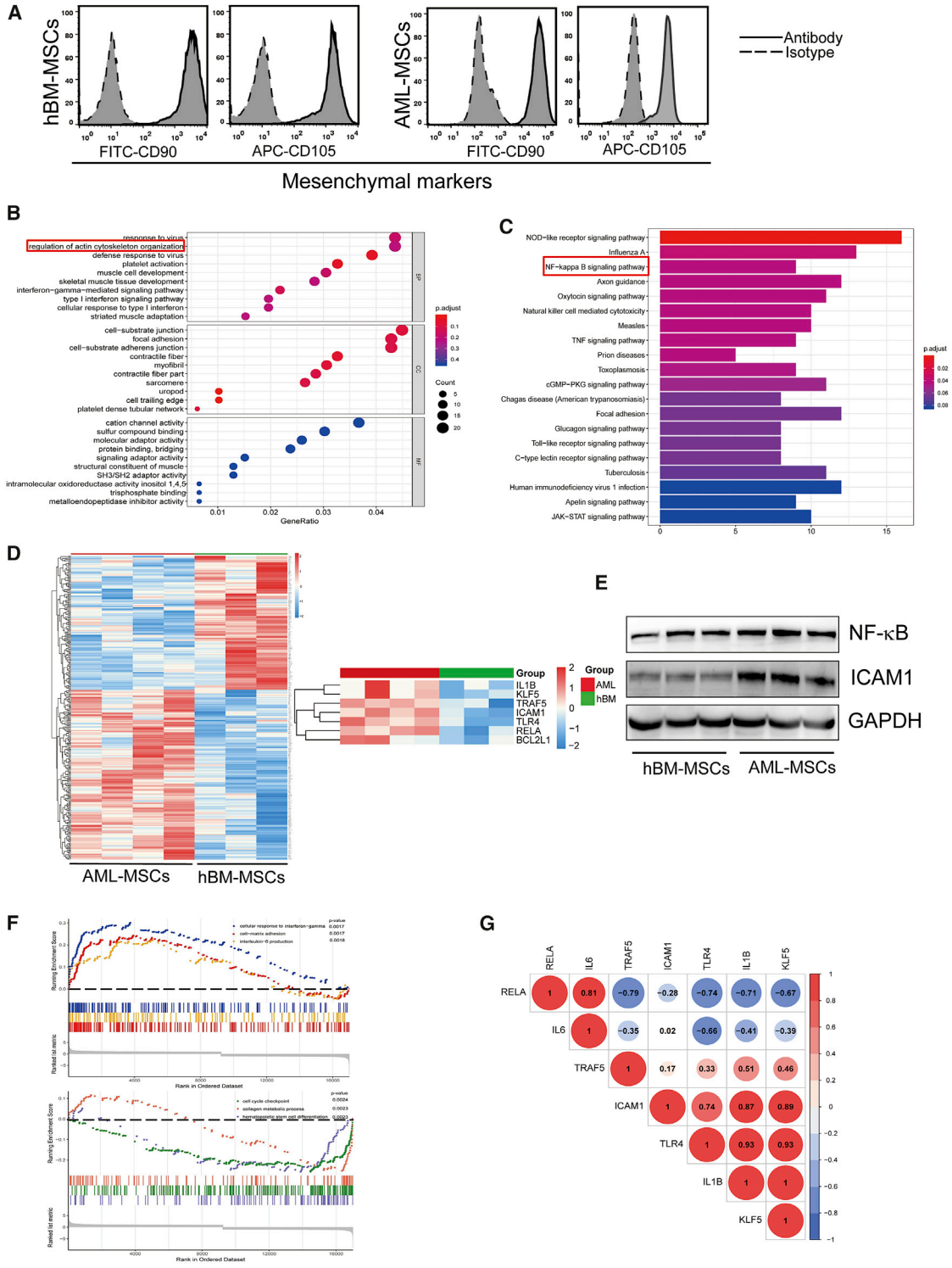

Figure 1. Gene Expression Patterns of MSCs Are Explored Between Healthy Donors and AML Patients

(A) hBM-MSCs and AML-MSCs stained with CD90 and CD105 antibodies were subjected to flow cytometry evaluation. (B and C) GO (B) and KEGG (C) were used to describe gene set functions among the significant upregulated mRNAs (absolute $\log_2$FC $\geq$ 1 and $p < 0.05$). (D) The heatmap of significantly regulated genes is presented. (E) Western blot was subjected to detect p65/NF-κB and ICAM1 expression. (F) GSEA was performed comparing transcriptional profiles of hBM-MSCs and AML-MSCs. (G) Correlations of RELA, IL-6, TRAF5, ICAM1, TLR4, IL-1β, and KLF5 are displayed in AML-MSC gene expression files.

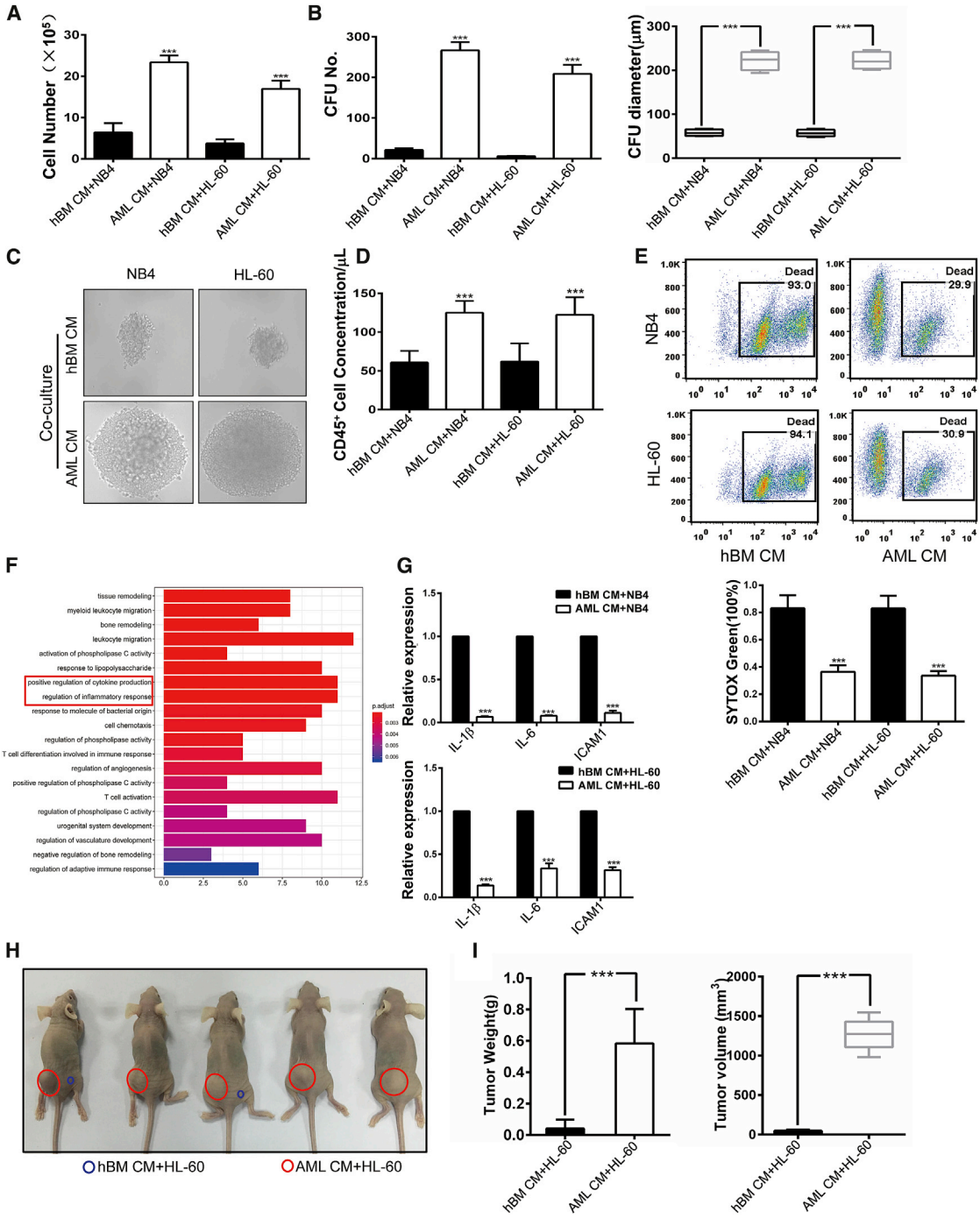

Figure 2. AML-MSCs Promote Proliferation and Colony Formation of Leukemic Cells

(A) NB4 and HL-60 cells were co-cultured with hBM-MSC CM or AML-MSC CM for 48 h and cell numbers were counted (mean ± SD; ***$p < 0.001$). (B) Cells were co-cultured with hBM-MSC CM or AML-MSC CM for 72 h and then cultured in semi-solid medium. The colony numbers and the diameters of colonies are shown (mean ± SD; ***$p < 0.001$). (C) Morphological changes of the colonies were observed under microscopy (original magnification, ×100). (D) Cells were co-cultured with hBM-MSCs or AML-MSCs for 48 h and the adherent cells were counted (mean ± SD; ***$p < 0.001$). (E) NB4 and HL-60 cells were co-cultured with hBM-MSC CM or AML-MSC CM for 6 days and subjected to Sytox Green stain. (F) GO was used to describe gene set functions between HL-60 cells co-cultured with hBM-MSCs or AML-MSCs. (G) NB4 and HL-60 cells were co-cultured with hBM-MSC CM or AML-MSC CM for 48 h and subjected to real-time PCR (mean ± SD; ***$p < 0.001$). (H and I) HL-60 cells were co-cultured with hBM-MSC CM or AML-MSC CM and injected into the flanks of nude mice. (H) A representative photograph is shown 3 weeks after injection, and (I) the weight and volume of tumors were measured (mean ± SD, n = 5; ***$p < 0.001$).

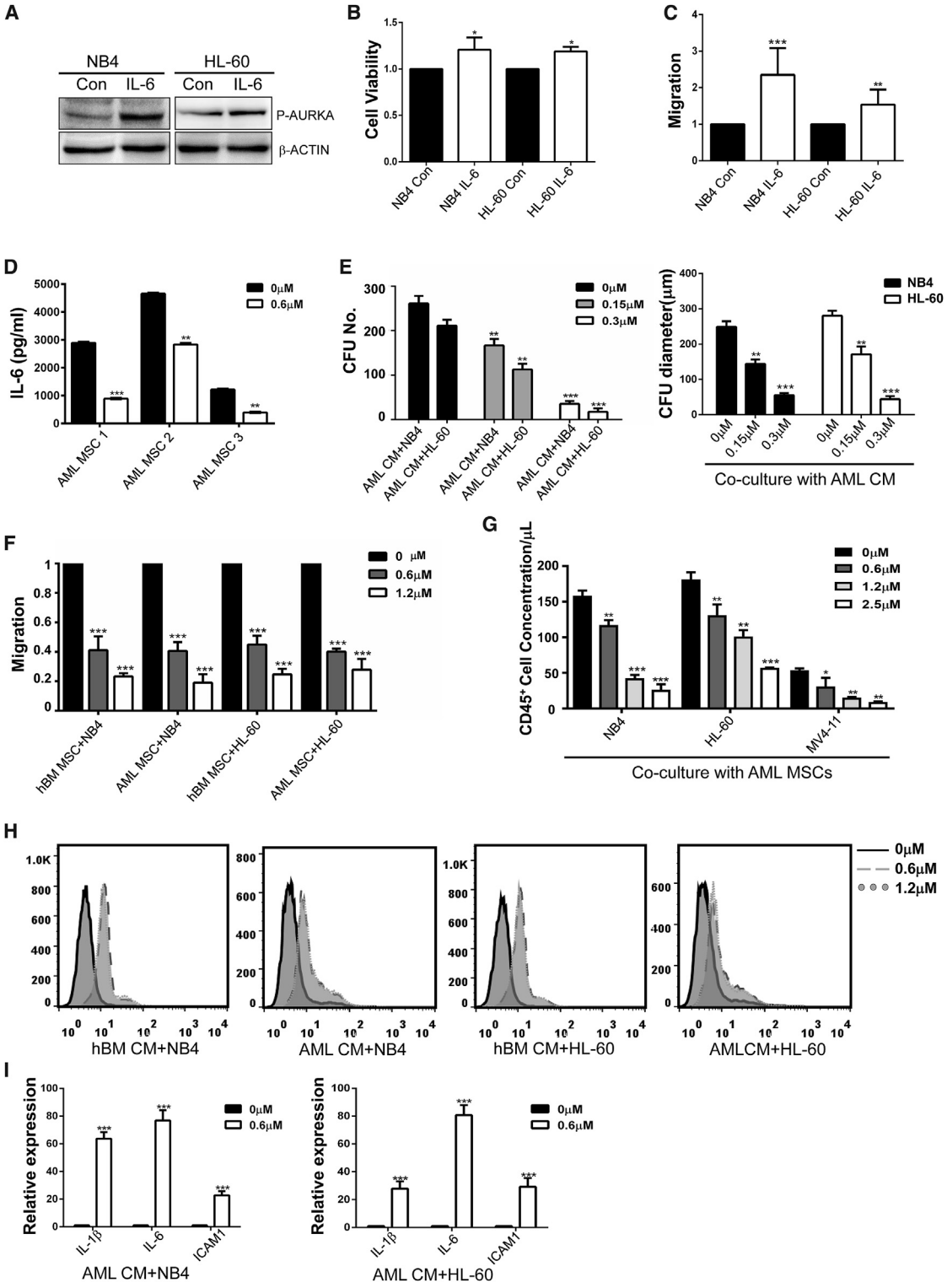

Figure 3. Inhibition of AURKA by PW21 Overcomes MSC-Induced Malignancies

(A) NB4 or HL-60 cells were treated with 50 ng/mL IL-6 and subjected to western blot for detection of AURKA phosphorylation. (B and C) Cells were treated with or without IL-6 and subjected to cell viability (B) and transwell assays (C). (D) An ELISA assay was applied to detect the IL-6 level in AML-MSC CM treated with PW21 or not (mean ± SD;

(legend continued on next page)

152.0 nM. Furthermore, PW21 was used to access the effect of inhibition of AURKA on AML-MSC-induced malignancy. We found that PW21 could greatly suppress IL-6 secretion by AML-MSCs (Figure 3D) and decrease the AML-MSC-induced CFU in NB4 and HL-60 cells (Figure 3E). Similarly, PW21 decreased the cell adhesion and migration induced by AML-MSCs significantly (Figures 3F and 3G). Additionally, a carboxyfluorescein succinimidyl ester (CFSE) assay showed that PW21 inhibited the high proliferated cells both when co-cultured with AML-MSC or hBM-MSC CM (Figure 3H). Real-time PCR revealed that ICAM1, IL-6, and IL-1β were all increased after PW21 treatment in AML-MSC CM co-cultures (Figure 3I), suggesting the different biologic function of ICAM1, IL-6, and IL-1β in leukemic cells. Our data implied that PW21 might have a potential therapeutic application in leukemia treatment by interfering with the AML environment.

PW21 Induces Cell Cycle Arrest and Apoptosis as well as Inhibits the Growth of Leukemic Cells *In Vivo*

Next, we showed that mechanism of PW21 in suppressing leukemic cells. A CFU assay showed that PW21 greatly decreased the number and the diameter of colonies in a dose-dependent manner in NB4, HL-60, and MV4-11 cells as well as retinoic acid-resistant NB4-R2 cells (Figure 4A) without MSC co-culture. A CFSE assay also showed that PW21 significantly inhibited cell proliferation (Figure 4B). Due to the crucial role of AURKA in mitosis, the cell cycle blocking effect on NB4 and HL-60 cells was examined. PW21 greatly induced G_2/M cell cycle arrest and polyploidization in AML cells (Figure 4C). An immunofluorescence assay further confirmed that PW21 induced polyploidy in cells (Figure 4D). Moreover, CRISPR-Cas9 was applied to knock out AURKA expression in leukemic cells and we found that AURKA deletion could reduce cell proliferation and adhesion induced by AML-MSCs, as well as induce cell cycle arrest and lead to cell death (Figures 4E–4H; Figures S3A–S3C), which was similar with PW21 treatment. Meanwhile, knockout IL-6 receptor expression in HL-60 cells also promoted cell death when culture with AML-MSC CM, further demonstrating that IL-6 signaling was of great importance in maintaining leukemic cell survival (Figure S3D).

Previous reports revealed that AURKA inhibitors could inhibit cell proliferation but not induce obvious apoptosis.[13,14] Our new designed PW21 not only suppressed cell proliferation (Figure 5A), but it also promoted significant cell apoptosis in NB4, HL-60, MV4-11, and NB4-R2 cells (Figure 5B). However, PW21 displayed less toxicity to normal peripheral blood mononuclear cells (Figure S4). Mechanically, PW21 inhibited AURKA activation and induced caspase-8 and poly(ADP-ribose) polymerase (PARP) cleavage, associated with a decrease of mitogen-activated protein kinase (MAPK) phosphorylation (Figure 5C). Additionally, PW21 decreased nuclear NF-κB expression strongly (Figures 5D and 5E). These results suggested that the proliferative inhibition induced by PW21 could be associated with cell cycle blockage and apoptosis mediated by NF-κB signaling. Furthermore, PW21 increased IL-6 and IL-1β expression (Figure 5F), consistent with the results in MSC CM co-culture. Luciferase-labeled NB4 or HL-60 cells were treated PW21, and the result revealed that inhibition of AURKA clearly reduced the bioluminescence (Figure 5G). To evaluate the role of PW21 in the development of leukemia *in vivo*, we transplanted luciferase-labeled HL-60 cells into non-obese diabetic (NOD)-severe combined immunodeficiency (SCID) mice and then treated the mice with PW21. Lower bioluminescence signal intensity was observed in mice that received PW21 compared with those treated with vehicle (Figure 5H), suggesting a therapeutic benefit of inhibiting AURKA pathways.

PW21 Delays Leukemia Progression

Considering that the high expression level of AURKA might contribute to leukemic progression, we used an MLL-AF9-mediated murine model to study PW21 in AML development. We transduced the MLL-AF9 fusion gene to the murine BMs, which were transplanted to the recipient mice to develop leukemia. Then the BMs were collected and the GFP^+ BMs were used for apoptosis and a CFU assay (Figure 6A). As shown in Figure 6B, PW21 could reduce the number and diameter of colonies in GFP^+ BMs greatly. Similarly, PW21 induced apoptotic cell death and cell cycle arrest in G_2/M as indicated in cell lines (Figures 6C and 6D). Then, the BMs were further used for a second transplantation. After transplantation, the mice were treated intragastrically with vehicle or PW21 every 2 days. We found a significantly prolonged lifespan of MLL-AF9 leukemic mice after treatment with PW21 (Figure 6E). Morphological analysis showed that more leukemic blast cells with segmented nuclei were present in the PW21 group (Figure 6F). The splenomegaly in MLL-AF9 leukemic mice was relieved in the PW21 group, as evidenced by a remarkably smaller size and decreased spleen weight compared with the control group (Figure 6G). Flow cytometric analysis also showed decreased expression of GFP^+ cells or $GFP^+c\text{-}Kit^+Gr\text{-}1^-$ cells in the PW21-treated group (Figures 6H and 6I). In addition, increased expression of Gr-1 was detected in the PW21 group, indicating that PW21 might promote the differentiation of MLL-AF9 leukemia cells (Figure 6I). These data demonstrated that PW21 was critical for inducing a differentiated phenotype and suppressing leukemic progression.

DISCUSSION

Most recent therapeutic approaches have shifted from targeting leukemic cells to interfering with the microenvironment, as the influence on the leukemic microenvironment has been clearly shown to be pivotal in leukemic cell chemoresistance. The presence of MSCs

**p < 0.01, ***p < 0.001). (E) Cells were co-cultured with AML-MSC CM for 72 h and then cultured in semi-solid medium and treated with or without PW21; colony numbers and the diameters of colonies are shown (mean ± SD; **p < 0.01, ***p < 0.001). (F and G) Cells were co-cultured with hBM-MSCs or AML-MSCs with or without PW21 and subjected to a transwell assay (F) or adhesion assay (G). (H and I) A CFSE assay (H) and real-time PCR detection (I) were used to analyze in cells co-cultured with hBM-MSC CM or AML-MSC CM with or without PW21 for 48 h.

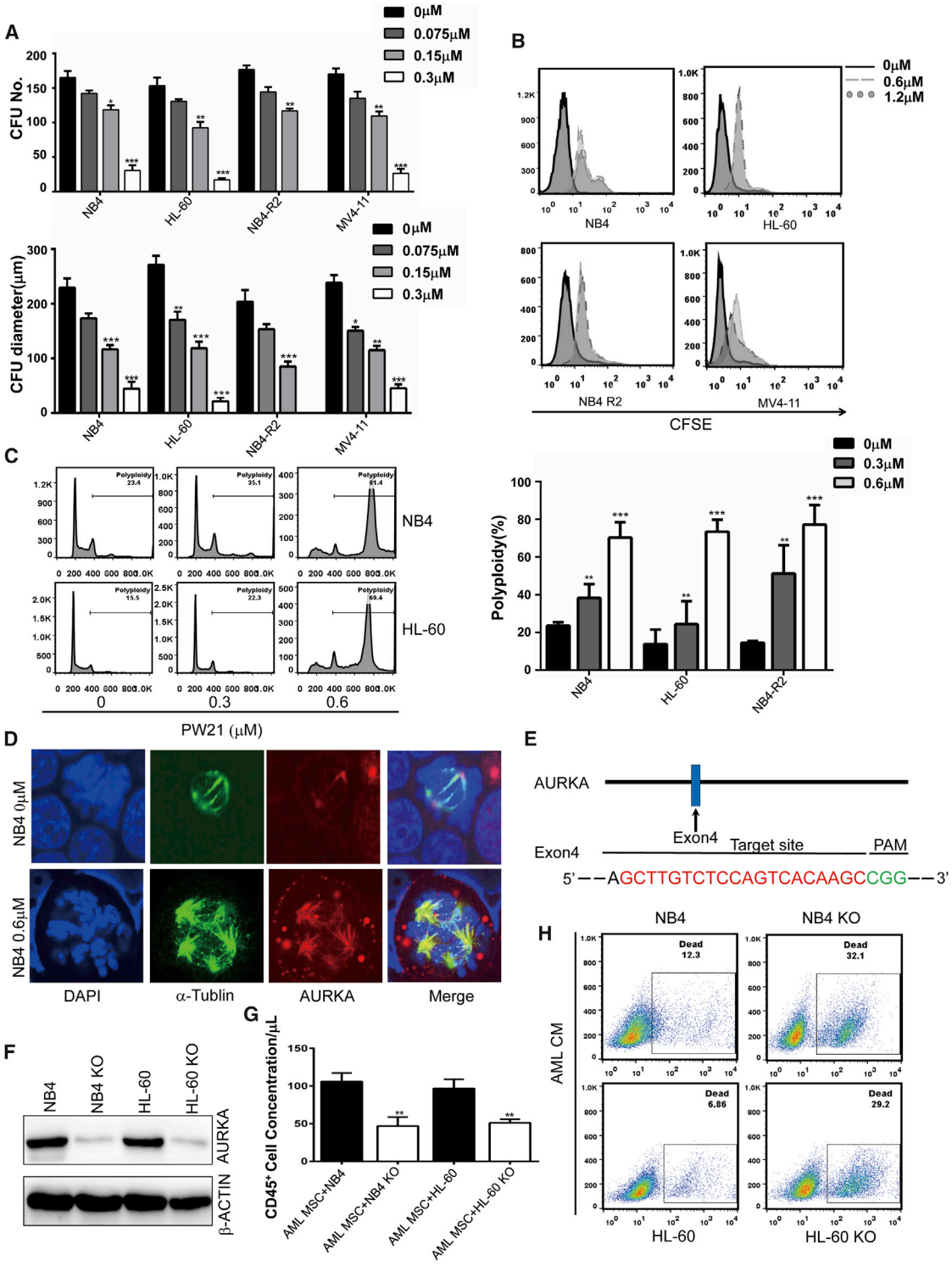

Figure 4. PW21 Induces Cell Cycle Arrest and Polyploidy

(A) NB4, HL-60, NB4 R2, and MV4-11 cells treated with or without PW21 were cultured in semi-solid medium, and the colony numbers and the diameters of colonies are shown (mean ± SD; *$p < 0.05$, **$p < 0.01$, ***$p < 0.001$). (B–D) Cells were treated with or without PW21 for 48 h and subjected to a CFSE assay (B) and cell cycle detection (C),

(legend continued on next page)

promotes leukemic cells to escape from apoptosis, and leukemia development is often associated with persistent abnormalities in the microenvironment. Wnt/β-catenin, sonic hedgehog, and Notch pathways play an important role in the crosstalk between leukemic cells and the stromal microenvironment.[17,18]

Among the stromal microenvironment, MSCs activated a wide variety of signaling pathway, supporting the survival of leukemic cells, and only a few investigations have shown the signal profiles of MSCs from leukemia patients. In agreement with previous studies, our data showed that different cell adhesion molecules and cytokines were expressed by MSCs between normal donors and patients, indicating the possibility of crosstalk between the leukemic cells and microenvironment. We demonstrated that AML-MSCs showed higher expression of ICAM1 compared to hBM-MSCs, along with aberrant cytokine activation in the NF-κB pathway (Figure 1). ICAM1 is an adhesion molecule, which was expressed in MSCs and contributed to drug resistance of leukemic cells.[19,20] In parallel, we observed that AML-MSCs promoted leukemic cell proliferation, colony formation and migration, protecting leukemic cells from apoptosis (Figure 2), which suggested that adhesion molecules and cytokines expressed by MSCs were of importance to offer leukemic cells a sustaining microenvironment.

Considerable evidence supported the existence of cytokine deregulation in cancer patients that might be associated with pathogenesis, disease progression, and patient survival. For example, IL-6 provided extrinsic protection for several solid tumors and leukemia. The plasma IL-6 level was higher in AML patients from both groups of age and was associated with patient survival and event-free survival.[21] In pediatric AML, IL-6-induced signal transducer and activator of transcription 3 (STAT3) signaling was activated frequently at relapse, and it was associated with inferior survival after relapse, suggesting that the IL-6 pathway could represent a target for overcoming environment-mediated chemotherapy resistance.[22] In CLL, MSCs supported the survival of leukemic cells *in vitro* through an IL-6-dependent mechanism.[23] In MM, upregulation of IL-6 by MSCs led to the acquisition of resistance to the chemotherapeutic agent.[24] Moreover, the MM-derived macrophage migratory inhibitory factor caused IL-6 secretion via c-MYC to accelerate disease progression.[25] In CML, IL-6 was a novel biomarker, with high diagnostic plasma levels strongly predictive of subsequent failure to achieve early molecular response and deep molecular response, as well as transformation to blast crisis.[26] All of this evidence demonstrated that IL-6 in the leukemic microenvironment sustained the survival of leukemic cells, resulting in poor prognosis.

Strikingly, we found that IL-6 secreted from microenvironment could enhance AURKA activation in leukemic cells and improve cell proliferation and migration (Figures 3A–3C). Since AURKA was dysregulated in different tumor types, including leukemia,[3,27,28] AURKA inhibitors attracted great attention in leukemia therapy. In the present study, we found that the novel AURKA inhibitor PW21 could inhibit IL-6 secretion by MSCs (Figure 3D). Importantly, PW21 inhibited MSC-induced cell proliferation, adhesion, and migration (Figures 3E–3H), indicating that the AURKA inhibitor could overcome drug resistance induced by IL-6 from the leukemic microenvironment. We and others also reported that AURKA overexpression contributed to NF-κB activation,[16,29,30] and IL-6 could activate NF-κB.[15] Thus, IL-6-induced NF-κB expression might be mediated though AURKA in leukemic cells. The AURKA inhibitor could be a potential choice to target leukemic cells and their environment while NF-κB signaling is activated.

Interestingly, leukemic cells cultured with CM from AML-MSCs presented reduced IL-6 and IL-1β expression compared with the hBM-MSC group (Figures 2F and 2G). Also, PW21 greatly increased IL-6 and IL-1β expression in leukemic cells with or without AML-MSC CM co-culture (Figures 3I and 5F). IL-1β, a pro-inflammatory cytokine, which was generated from inflammatory umbilical cord-derived MSCs, promoted stem cell-like characteristics of cancer cells.[31] On the contrary, IL-1β inhibited self-renewal capacity in dormant $CD34^+/CD38^-$ AML cells.[32] IL-1β was also increased after treatment with arsenic trioxide or all-*trans* retinoic acid.[33,34] Similarly, IL-6 displayed opposing effects on cancer cells.[35] For instance, in a phosphatase and tensin homolog (PTEN)-deficient prostate cancer model, IL-6/STAT3 signaling in tumor cells protected against tumor progression.[36] In addition, a study showed a decreased expression of IL-1β and IL-6 in the leukocytes of lymphocytic leukemia patients,[37,38] providing support that IL-1β and IL-6 might display different functions in leukemic cells, which was context-dependent. Therefore, activation of IL-6 signaling in the environment promoted leukemic malignancies while inhibition of AURKA by PW21 increased IL-6 expression to induce cell death. This differential switch in shared IL-6 signaling pathways required an attractive molecular explanation for the opposing pro-tumorigenic and anti-tumorigenic activities.

In vivo, we investigated the effect of PW21 by using the NOD-SCID model and MLL-AF9 leukemic model. Our results showed that PW21 significantly inhibited the growth of leukemic cells and delayed the disease progression (Figures 5H and 6E–6G). Mechanically, PW21 arrested the cell cycle in the G_2/M phase and induced MLL-AF9 leukemic cell apoptosis (Figures 6C and 6D). PW21 could suppress GFP^+ leukemic cells and induce Gr-1 expression (Figures 6H and 6I), consistent with our previous reports that the AURKA inhibitor could promote cell differentiation.[14] Since activation of metabolic signaling pathways by inducing polyploidy could be specific to leukemic cell survival,[39,40] a better understanding of the underlying mechanism of PW21-induced polyploidy will be important as AURKA inhibitors progress toward clinical development.

as well as immunofluorescent staining of tubulin and AURKA (D). (E) AURKA was knocked out in NB4 and HL-60 cells by CRISPR-Cas9. (F) Western blot was subjected to detect AURKA expression. (G) Cells were co-cultured with AML-MSCs for 48 h and subjected to an adhesion assay (mean ± SD; $^{**}p < 0.01$). (H) Sytox Green stain assay was applied to detect cells with AML-MSC CM co-culture for 48 h.

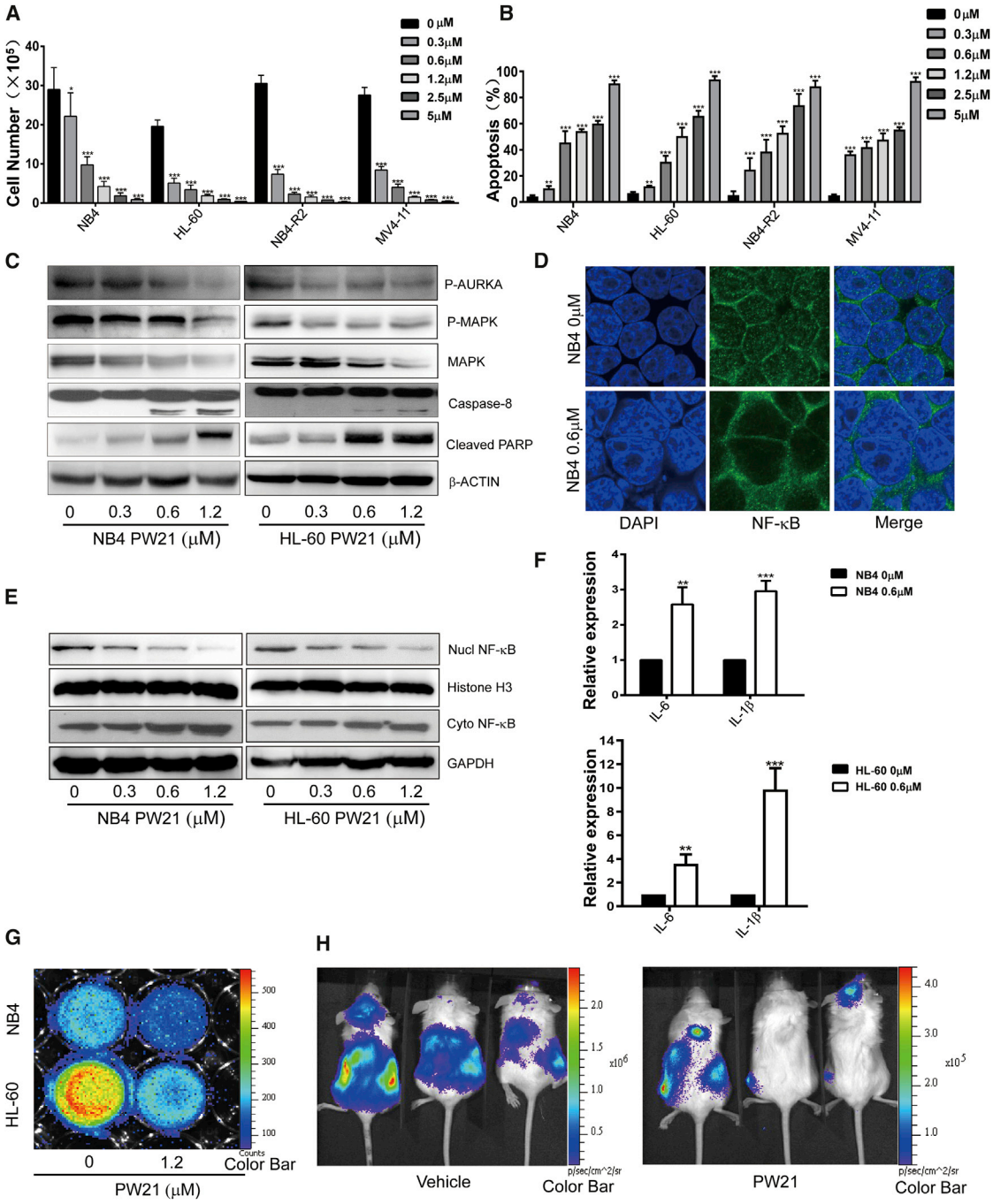

Figure 5. PW21 Induces Apoptosis and Inhibits the Growth of Leukemic Cells *In Vivo*

(A–E) Cells were treated with or without PW21 for 48 h and subjected to a cell counting assay (A), apoptosis detection (B), western blot of apoptotic-related proteins (C), immunofluorescent staining of p65/NF-κB (D), and western blot of p65/NF-κB (E). (F) Real-time PCR was subjected to detect gene expression (mean ± SD; $^{**}p < 0.01$, $^{***}p < 0.001$). (G) Luciferase-red fluorescent cells treated with or without PW21 for 48 h and imaged. (H) Luciferase-red fluorescent-labeled NOD-SCID mice were injected intraperitoneally with D-luciferin and imaged after treatment with PW21 for 2 weeks.

In summary, we showed that targeting AURKA by PW21 not only inhibited leukemic cell proliferation and induced apoptosis, but also overcame the protection induced by IL-6 from MSCs in the leukemic microenvironment. Our results provided a new approach for treatment of leukemia by dual-targeting leukemic cells and microenvironments via AURKRA inhibition in clinical application.

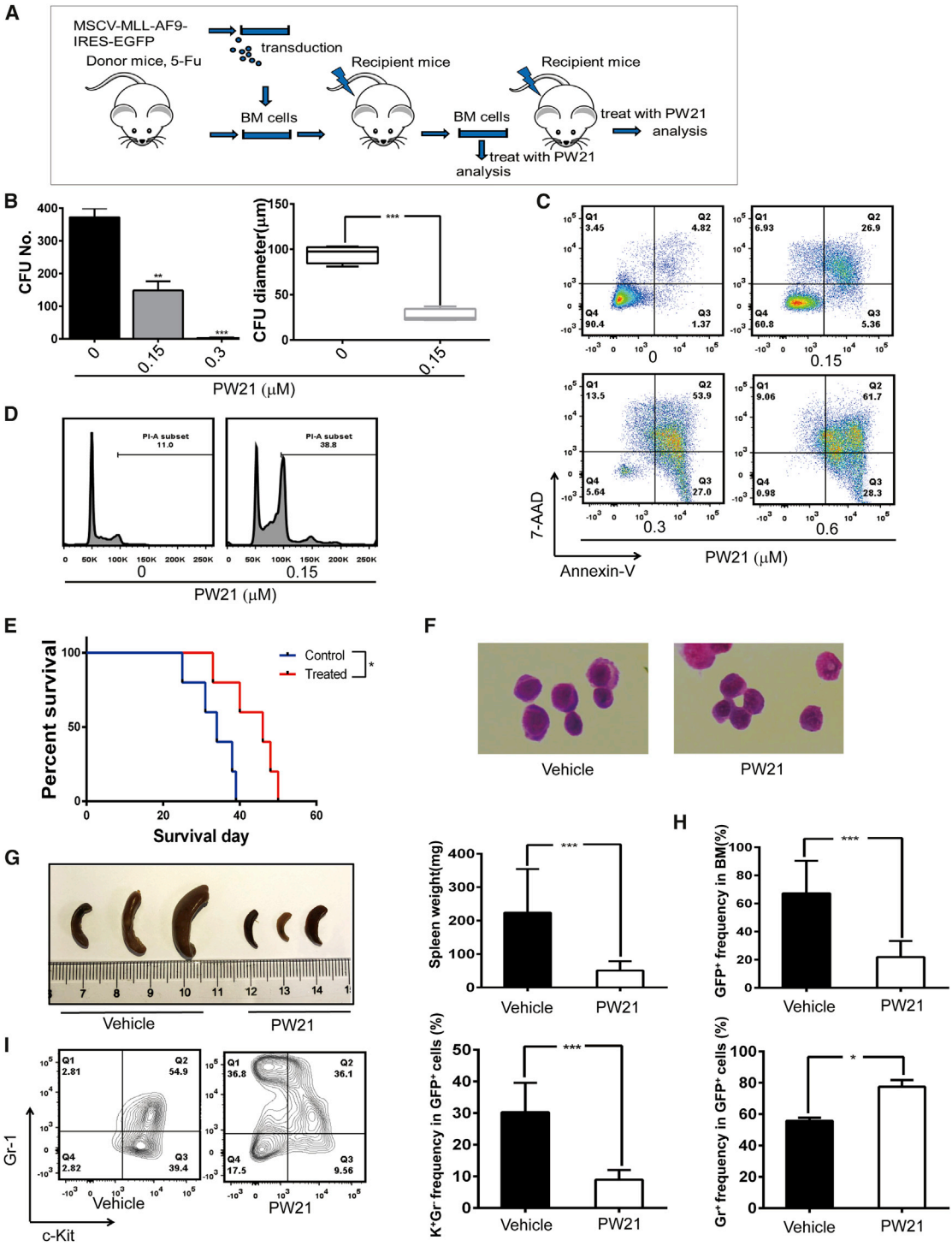

Figure 6. PW21 Delays Leukemia Progression

(A) Chart of the treatment procedure for leukemic model. (B) GFP$^+$ BM cells collected from the MLL-AF9 transplanted mice were treated with or without PW21 and cultured in semi-solid medium, and the colony numbers and the diameters of colonies are shown (mean ± SD; $^{**}p < 0.01$, $^{***}p < 0.001$). (C and D) GFP$^+$ BM cells were treated with or without PW21 for 48 h and subjected to apoptosis (C) and cell cycle detection (D). (E) After the BM cells were transplanted, the mice were treated with or without PW21 for 2 weeks, and Kaplan-Meier plots of survival were analyzed. (F) Wright-Giemsa staining was measured in the PW21-treated group and control group. (G) Spleens were

(legend continued on next page)

MATERIALS AND METHODS

Patients and Samples

MSCs were obtained from BMs of healthy donors and untreated AML patients at the Department of Hematology, The Third Affiliated Hospital of Sun Yat-sen University, following written informed consent according to the Declaration of Helsinki. The study was approved by the Institute Research Ethics Committee at The Third Affiliated Hospital of Sun Yat-sen University.

Reagents and Cell Cultures

AURKA inhibitor PW21 was designed and synthesized in our laboratory with a solution of 100 mM in DMSO. Leukemic cells were cultured in RPMI 1640 (Gibco, Grand Island, NY, USA) containing appropriate antibiotics and 10% fetal bovine serum (FBS, Gibco, Grand Island, NY, USA). HL-60, NB4-R2, and NB4 cells were provided by the Shanghai Institute of Hematology, Ruijin Hospital. MV4-11 was obtained from the American Type Culture Collection (ATCC, Manassas, VA, USA). MSCs were cultured in DMEM with 1g/L D-glucose (Gibco, Grand Island, NY, USA) containing appropriate antibiotics and 10% FBS. CM was collected by culturing MSCs with DMEM with 10% FBS for 48 h.

Measurement of Cell Death

After collecting and washing twice with PBS, cells were stained with annexin V-fluorescein isothiocyanate (FITC)/propidium iodide (PI), annexin V-phycoerythrin (PE)/7-aminoactinomycin D (7AAD), or Sytox according to the protocol (Thermo Fisher Scientific, Waltham, MA, USA). The samples were then subjected to flow cytometry evaluation.

Protein Expression and Localization

For western blot analysis, cells lysate concentration was determined by the Bradford method with BSA (Sigma, St. Louis, MO, USA) as the standard. Equal amounts of protein from each sample were subjected to electrophoresis in SDS-polyacrylamide gel and transferred to a nitrocellulose membrane (Millipore, Billerica, MA, USA). The membrane was blocked and then incubated with primary antibodies against GAPDH, β-actin, phosphorylated AURKA (p-AURKA), phosphorylated MAPK (p-MAPK), MAPK, cleaved PARP, caspase-8, NF-κB, ICAM1, and histone H3 (Cell Signaling Technology, Beverly, MA, USA) overnight at 4°C followed by incubation for 1 h at room temperature with appropriate secondary antibodies. Antibody binding was detected with an enhanced chemiluminescence kit.

The IL-6 levels in culture media were determined by human IL-6 ELISA Kit (R&D Systems, Minneapolis, MN, USA) following the manufacturer's instruction.

For immunofluorescence, NB4 cells were fixed with 4% paraformaldehyde and incubated with Triton X-100. Following incubation, the cells were blocked with PBS containing 5% BSA for 1 h and incubated with anti-AURKA antibody or anti-tubulin antibody at 37°C for 1 h. After washing with PBS, the cells were stained with second antibodies for 1 h. Then, the cells were stained with DAPI for 10 min. The images were observed under confocal microscopy at ×1,000 magnification.

Real-Time PCR

Total RNA was isolated by using TRIzol reagent (Thermo Fisher Scientific, Waltham, MA, USA), and the first-strand cDNA was then used as templates to detect the expression of the genes by an Applied Biosystems 7500 Fast real-time PCR system. The primers are listed in Table S1.

CFU Assay

Cells were plated in methylcellulose (R&D Systems, Minneapolis, MN, USA) and treated with CM or PW21. On the indicated day after plating, the CFU were counted.

Adhesion and Migration Assays

For adhesion, MSCs were plated in six-well plates and cultured for 24 h. Then, leukemic cells were cultured on the surface of MSCs for another 48 h with or without PW21. Attached leukemic cells were counted by flow cytometry after staining with human CD45 MicroBeads (Miltenyi Biotec, Germany) in the presence of CountBright absolute counting beads (Thermo Fisher Scientific, Waltham, MA, USA). Adhesion capability was defined according to the manufacturer's instructions.

For migration, MSCs were plated in the lower chamber of transwell plates and cultured for 24 h. Leukemic cells were added in the insert and cultured for another 12 h with or without PW21. The cell number of migration was defined as viable cells in the lower chamber.

Affymetrix GeneChip

A high-throughput Clariom S array (Affymetrix) was performed on normal MSCs and AML MSCs or HL-60 cultured with CM from hBM-MSCs and AML-MSCs, and analyzed with Limma in the R platform.

CRISPR-Cas9-Mediated Gene Editing in AML Cells

AML cells were infected with LentiCRISPRv2 lentivirus with the target sites of AURKA or IL-6 receptor sequence. Infected clones were selected with puromycin (Thermo Fisher Scientific, Waltham, MA, USA) for further analysis.

Tumor Growth in Xenografts

HL-60 cells were incubated with leukemic MSC CM or normal MSC CM for 48 h and then injected into the flanks of female BALB/c nude mice. Tumor volumes were calculated by the following formula: A ×

obtained from the PW21-treated group and control group. (H) Flow cytometry results of GFP expression from the BM cells in the PW21-treated group and control group are shown (mean ± SD, n = 3; ***$p < 0.001$). (I) Flow cytometry results of Gr-1 and c-Kit expression from the GFP^+ BM cells in the PW21-treated group and control group are presented (mean ± SD, n = 3; *$p < 0.05$, ***$p < 0.001$).

$B^2/2$, where A is the greatest diameter and B is the diameter perpendicular to A. Other indicators of general health, such as body weight, feeding behavior, and motor activity of each animal, were also monitored. After the animals were euthanized, tumor xenografts were immediately removed and weighed. All animal studies were approved by The Third Affiliated Hospital of Sun Yat-sen University Animal Care and Use Committee.

Bioluminescence Imaging

For bioluminescence imaging assay, NOD-SCID mice were intravenously transplanted with luciferase-labeled HL-60 cells. Luciferase red fluorescent protein plasmid was provided by Prof. Xiaofeng Zhu at Sun Yat-sen University Cancer Center. 7 days after transplantation, the mice were treated intragastrically with vehicle or PW21 every 2 days at a dose of 50 mg per kg of body weight. Then, the mice were injected intraperitoneally with 150 mg/kg D-luciferin and imaged with the *in vivo* imaging system (IVIS) Lumina system (PerkinElmer, Waltham, MA, USA). All animal studies were approved by The Third Affiliated Hospital of Sun Yat-sen University Animal Care and Use Committee.

BM Infection and Transplantation

293FT cells were transfected with retroviral vectors MSCV-MLL-AF9-IRES-EGFP for virus packaging. BM from 5-fluorouracil (5-FU)-treated donor mice was transduced with MLL-AF9 retrovirus in the presence of IL-3, IL-6, and stem cell factor (SCF). Wild-type recipient mice were irradiated by X-ray and transplanted with MLL-AF9-transduced cells via tail vein injection. Diseased mice were analyzed by histopathological and biochemical examination. The BMs from the diseased mice were then collected for analysis or transplanted to the second recipient mice before being treated with or without PW21 at a dose of 50 mg per kg of body weight. All animal studies were approved by The Third Affiliated Hospital of Sun Yat-sen University Animal Care and Use Committee.

Statistical Analysis

Statistics were calculated by GraphPad Prism software (version 6.0). Differences among variables were assessed by an unpaired Student's t test between two groups and by ANOVA with multiple comparisons. The level of significance was set at $p < 0.05$.

SUPPLEMENTAL INFORMATION

Supplemental Information can be found online at https://doi.org/10.1016/j.omto.2020.08.001.

AUTHOR CONTRIBUTIONS

Z.-J.L. and Q.L. designed the experiments and reviewed the manuscript; J.-D.W., W.Z., L.Z., J.-W.Z., and L.-X.W. conducted the experiments and reviewed the manuscript; G.L. and L.L. designed and synthesized PW21. J.-D.W. and H.-S.Z. participated in writing the manuscript. All authors read and approved the final manuscript.

CONFLICTS OF INTEREST

The authors declare no competing interests.

ACKNOWLEDGMENTS

We thank Dr. Ze-Xiu Xiao in The Third Affiliated Hospital, Sun Yat-sen University for technologic support. This study was supported by the National High Technology Research and Development Program of China (863 Program; no. 2015AA020926 to Z.-J.L.); the National Natural Science Foundation of China (no. 81630005 to Q.L.); the Guangdong Basic and Applied Basic Research Foundation (nos. 2018A030313071 and 2019A1515011185 to Z.-J.L.); the Science and Technology Planning Project of Guangzhou (nos. 202002030461 to Z.-J.L. and 201804020044 to Q.L.); and by the Fundamental Research Funds for the Central Universities (no. 18ykzd01 to Z.-J.L.).

REFERENCES

1. Sun, Z., Wang, S., and Zhao, R.C. (2014). The roles of mesenchymal stem cells in tumor inflammatory microenvironment. J. Hematol. Oncol. *7*, 14.
2. Lee, M.W., Ryu, S., Kim, D.S., Lee, J.W., Sung, K.W., Koo, H.H., and Yoo, K.H. (2019). Mesenchymal stem cells in suppression or progression of hematologic malignancy: current status and challenges. Leukemia *33*, 597–611.
3. Goldenson, B., and Crispino, J.D. (2015). The aurora kinases in cell cycle and leukemia. Oncogene *34*, 537–545.
4. Huang, X.F., Luo, S.K., Xu, J., Li, J., Xu, D.R., Wang, L.H., Yan, M., Wang, X.R., Wan, X.B., Zheng, F.M., et al. (2008). Aurora kinase inhibitory VX-680 increases Bax/Bcl-2 ratio and induces apoptosis in Aurora-A-high acute myeloid leukemia. Blood *111*, 2854–2865.
5. von der Heide, E.K., Neumann, M., Vosberg, S., James, A.R., Schroeder, M.P., Ortiz-Tanchez, J., Isaakidis, K., Schlee, C., Luther, M., Jöhrens, K., et al. (2017). Molecular alterations in bone marrow mesenchymal stromal cells derived from acute myeloid leukemia patients. Leukemia *31*, 1069–1078.
6. Oliveira, F.M., Lucena-Araujo, A.R., Favarin, Mdo.C., Palma, P.V., Rego, E.M., Falcão, R.P., Covas, D.T., and Fontes, A.M. (2013). Differential expression of *AURKA* and *AURKB* genes in bone marrow stromal mesenchymal cells of myelodysplastic syndrome: correlation with *G-banding* analysis and FISH. Exp. Hematol. *41*, 198–208.
7. Lucena-Araujo, A.R., de Oliveira, F.M., Leite-Cueva, S.D., dos Santos, G.A., Falcao, R.P., and Rego, E.M. (2011). High expression of *AURKA* and *AURKB* is associated with unfavorable cytogenetic abnormalities and high white blood cell count in patients with acute myeloid leukemia. Leuk. Res. *35*, 260–264.
8. Yan, M., Wang, C., He, B., Yang, M., Tong, M., Long, Z., Liu, B., Peng, F., Xu, L., Zhang, Y., et al. (2016). Aurora-A kinase: a potent oncogene and target for cancer therapy. Med. Res. Rev. *36*, 1036–1079.
9. Görgün, G., Calabrese, E., Hideshima, T., Ecsedy, J., Perrone, G., Mani, M., Ikeda, H., Bianchi, G., Hu, Y., Cirstea, D., et al. (2010). A novel Aurora-A kinase inhibitor MLN8237 induces cytotoxicity and cell-cycle arrest in multiple myeloma. Blood *115*, 5202–5213.
10. Kelly, K.R., Ecsedy, J., Medina, E., Mahalingam, D., Padmanabhan, S., Nawrocki, S.T., Giles, F.J., and Carew, J.S. (2011). The novel Aurora A kinase inhibitor MLN8237 is active in resistant chronic myeloid leukaemia and significantly increases the efficacy of nilotinib. J. Cell. Mol. Med. *15*, 2057–2070.
11. Qi, W., Spier, C., Liu, X., Agarwal, A., Cooke, L.S., Persky, D.O., Chen, D., Miller, T.P., and Mahadevan, D. (2013). Alisertib (MLN8237) an investigational agent suppresses Aurora A and B activity, inhibits proliferation, promotes endo-reduplication and induces apoptosis in T-NHL cell lines supporting its importance in PTCL treatment. Leuk. Res. *37*, 434–439.
12. Goldberg, S.L., Fenaux, P., Craig, M.D., Gyan, E., Lister, J., Kassis, J., Pigneux, A., Schiller, G.J., Jung, J., Jane Leonard, E., et al. (2014). An exploratory phase 2 study of investigational Aurora A kinase inhibitor alisertib (MLN8237) in acute myelogenous leukemia and myelodysplastic syndromes. Leuk. Res. Rep. *3*, 58–61.
13. Wang, L.X., Wang, J.D., Chen, J.J., Long, B., Liu, L.L., Tu, X.X., Luo, Y., Hu, Y., Lin, D.J., Lu, G., et al. (2016). Aurora A kinase inhibitor AKI603 induces cellular senescence in chronic myeloid leukemia cells harboring T315I mutation. Sci. Rep. *6*, 35533.

14. Long, Z.J., Wang, L.X., Zheng, F.M., Chen, J.J., Luo, Y., Tu, X.X., Lin, D.J., Lu, G., and Liu, Q. (2015). A novel compound against oncogenic Aurora kinase A overcomes imatinib resistance in chronic myeloid leukemia cells. Int. J. Oncol. *46*, 2488–2496.

15. De Simone, V., Franzè, E., Ronchetti, G., Colantoni, A., Fantini, M.C., Di Fusco, D., Sica, G.S., Sileri, P., MacDonald, T.T., Pallone, F., et al. (2015). Th17-type cytokines, IL-6 and TNF-α synergistically activate STAT3 and NF-kB to promote colorectal cancer cell growth. Oncogene *34*, 3493–3503.

16. Yao, J.E., Yan, M., Guan, Z., Pan, C.B., Xia, L.P., Li, C.X., Wang, L.H., Long, Z.J., Zhao, Y., Li, M.W., et al. (2009). Aurora-A down-regulates IkappaBα via Akt activation and interacts with insulin-like growth factor-1 induced phosphatidylinositol 3-kinase pathway for cancer cell survival. Mol. Cancer *8*, 95.

17. Zhang, B., Li, M., McDonald, T., Holyoake, T.L., Moon, R.T., Campana, D., Shultz, L., and Bhatia, R. (2013). Microenvironmental protection of CML stem and progenitor cells from tyrosine kinase inhibitors through N-cadherin and Wnt-β-catenin signaling. Blood *121*, 1824–1838.

18. Zhang, B., Ho, Y.W., Huang, Q., Maeda, T., Lin, A., Lee, S.U., Hair, A., Holyoake, T.L., Huettner, C., and Bhatia, R. (2012). Altered microenvironmental regulation of leukemic and normal stem cells in chronic myelogenous leukemia. Cancer Cell *21*, 577–592.

19. Reina, M., and Espel, E. (2017). Role of LFA-1 and ICAM-1 in cancer. Cancers (Basel) *9*, E153.

20. Wang, J., Liu, X., Qiu, Y., Shi, Y., Cai, J., Wang, B., Wei, X., Ke, Q., Sui, X., Wang, Y., et al. (2018). Cell adhesion-mediated mitochondria transfer contributes to mesenchymal stem cell-induced chemoresistance on T cell acute lymphoblastic leukemia cells. J. Hematol. Oncol. *11*, 11.

21. Sanchez-Correa, B., Bergua, J.M., Campos, C., Gayoso, I., Arcos, M.J., Bañas, H., Morgado, S., Casado, J.G., Solana, R., and Tarazona, R. (2013). Cytokine profiles in acute myeloid leukemia patients at diagnosis: survival is inversely correlated with IL-6 and directly correlated with IL-10 levels. Cytokine *61*, 885–891.

22. Stevens, A.M., Miller, J.M., Munoz, J.O., Gaikwad, A.S., and Redell, M.S. (2017). Interleukin-6 levels predict event-free survival in pediatric AML and suggest a mechanism of chemotherapy resistance. Blood Adv. *1*, 1387–1397.

23. Zhu, F., McCaw, L., Spaner, D.E., and Gorczynski, R.M. (2018). Targeting the IL-17/IL-6 axis can alter growth of chronic lymphocytic leukemia in vivo/in vitro. Leuk. Res. *66*, 28–38.

24. McNee, G., Eales, K.L., Wei, W., Williams, D.S., Barkhuizen, A., Bartlett, D.B., Essex, S., Anandram, S., Filer, A., Moss, P.A., et al. (2017). Citrullination of histone H3 drives IL-6 production by bone marrow mesenchymal stem cells in MGUS and multiple myeloma. Leukemia *31*, 373–381.

25. Piddock, R.E., Marlein, C.R., Abdul-Aziz, A., Shafat, M.S., Auger, M.J., Bowles, K.M., and Rushworth, S.A. (2018). Myeloma-derived macrophage inhibitory factor regulates bone marrow stromal cell-derived IL-6 via c-MYC. J. Hematol. Oncol. *11*, 66.

26. Nievergall, E., Reynolds, J., Kok, C.H., Watkins, D.B., Biondo, M., Busfield, S.J., Vairo, G., Fuller, K., Erber, W.N., Sadras, T., et al. (2016). TGF-α and IL-6 plasma levels selectively identify CML patients who fail to achieve an early molecular response or progress in the first year of therapy. Leukemia *30*, 1263–1272.

27. Kamran, M., Long, Z.J., Xu, D., Lv, S.S., Liu, B., Wang, C.L., Xu, J., Lam, E.W., and Liu, Q. (2017). Aurora kinase A regulates Survivin stability through targeting FBXL7 in gastric cancer drug resistance and prognosis. Oncogenesis *6*, e298.

28. Wan, X.B., Long, Z.J., Yan, M., Xu, J., Xia, L.P., Liu, L., Zhao, Y., Huang, X.F., Wang, X.R., Zhu, X.F., et al. (2008). Inhibition of Aurora-A suppresses epithelial-mesenchymal transition and invasion by downregulating MAPK in nasopharyngeal carcinoma cells. Carcinogenesis *29*, 1930–1937.

29. Briassouli, P., Chan, F., Savage, K., Reis-Filho, J.S., and Linardopoulos, S. (2007). Aurora-A regulation of nuclear factor-κB signaling by phosphorylation of IκBα. Cancer Res. *67*, 1689–1695.

30. Chefetz, I., Holmberg, J.C., Alvero, A.B., Visintin, I., and Mor, G. (2011). Inhibition of Aurora-A kinase induces cell cycle arrest in epithelial ovarian cancer stem cells by affecting NFκB pathway. Cell Cycle *10*, 2206–2214.

31. Luo, X., Huang, S., He, N., Liu, C., Chen, Y., Liu, Y., Mi, X., Li, N., Sun, P., Li, Z., et al. (2018). Inflammatory human umbilical cord-derived mesenchymal stem cells promote stem cell-like characteristics of cancer cells in an IL-1β-dependent manner. BioMed Res. Int. *2018*, 7096707.

32. Yang, J., Ikezoe, T., Nishioka, C., Nobumoto, A., and Yokoyama, A. (2013). IL-1β inhibits self-renewal capacity of dormant $CD34^{+}/CD38^{-}$ acute myelogenous leukemia cells in vitro and in vivo. Int. J. Cancer *133*, 1967–1981.

33. Dunoyer-Geindre, S., Rivier-Cordey, A.S., Tsopra, O., Lecompte, T., and Kruithof, E.K.O. (2017). Effect of ATRA and ATO on the expression of tissue factor in NB4 acute promyelocytic leukemia cells and regulatory function of the inflammatory cytokines TNF and IL-1β. Ann. Hematol. *96*, 905–917.

34. Gao, Y., Camacho, L.H., and Mehta, K. (2007). Retinoic acid-induced CD38 antigen promotes leukemia cells attachment and interferon-gamma/interleukin-1beta-dependent apoptosis of endothelial cells: implications in the etiology of retinoic acid syndrome. Leuk. Res. *31*, 455–463.

35. Jones, S.A., and Jenkins, B.J. (2018). Recent insights into targeting the IL-6 cytokine family in inflammatory diseases and cancer. Nat. Rev. Immunol. *18*, 773–789.

36. Pencik, J., Schlederer, M., Gruber, W., Unger, C., Walker, S.M., Chalaris, A., Marié, I.J., Hassler, M.R., Javaheri, T., Aksoy, O., et al. (2015). STAT3 regulated ARF expression suppresses prostate cancer metastasis. Nat. Commun. *6*, 7736.

37. Garley, M., Jabłońska, E., Sawicka-Powierza, J., Kłoczko, J., Piszcz, J., Kakareko, M., Ratajczak-Wrona, W., Charkiewicz, A., Omeljaniuk, W., and Szpak, A. (2016). Expression of IL-1 and IL-6 and their natural regulators in leukocytes of B-cell chronic lymphocytic leukaemia patients. Adv. Med. Sci. *61*, 187–192.

38. Allahbakhshian Farsani, M., Kamel, M., Mehrpouri, M., Heris, R.S., Hamidpour, M., Salari, S., and Mohamadi, M.H. (2020). The expression of interferon gamma (IFN-γ) and interleukin 6 (IL6) in patients with acute lymphoblastic leukemia (ALL). Pathol. Oncol. Res. *26*, 461–466.

39. Moreno-Sánchez, R., Rodríguez-Enríquez, S., Marín-Hernández, A., and Saavedra, E. (2007). Energy metabolism in tumor cells. FEBS J. *274*, 1393–1418.

40. Williams, B.R., Prabhu, V.R., Hunter, K.E., Glazier, C.M., Whittaker, C.A., Housman, D.E., and Amon, A. (2008). Aneuploidy affects proliferation and spontaneous immortalization in mammalian cells. Science *322*, 703–709.